Publ. Astron. Obs. Belgrade No. 91 (2012), 255 - 260 *Contributed paper*

SPECTRAL INDEX DISTRIBUTION OF RADIO AGNs: CASE STUDY OF 3C 349

V. BORKA JOVANOVIĆ[1], D. BORKA[1], R. SKEOCH[2] and P. JOVANOVIĆ[3]

[1] *Atomic Physics Laboratory (040), Vinča Institute of Nuclear Sciences, University of Belgrade, P.O. Box 522, 11001 Belgrade, Serbia*
E–mail: vborka@vinca.rs
E–mail: dusborka@vinca.rs

[2] *Department of Physics, University of York, Heslington, York, YO10 5DD, United Kingdom*
E–mail: ryan.skeoch@uniofyorkspace.net

[3] *Astronomical Observatory, Volgina 7, 11060 Belgrade, Serbia*
E–mail: pjovanovic@aob.rs

Abstract. We studied the spectral index distribution of radio Active Galactic Nuclei (AGNs) in the case of 3C 349. In our investigation, we used measurements of FR II radio galaxy 3C 349 at the two frequencies: 8415 and 1502 MHz, observed by the Very Large Array of the National Radio Astronomy Observatory. We estimated flux density profiles and spectral index map of 3C 349 and used them to discuss the structure of this extended radio source. We focused on the distribution of spectral indices over the jets and the lobes, as well as in their hotspots. We also calculated the mean value of flux density and compared it with earlier estimations.

1. INTRODUCTION

DRAGNs (Double Radio sources Associated with Galactic Nuclei) are large-scale double radio sources produced by outflows (jets) that are launched by processes in active galactic nuclei. Their main characteristics are synchrotron radiation, jets and lobes. This name was proposed by Leahy (1993) and includes the radio sources associated with radio galaxies, radio-loud quasars and some Seyfert galaxies.

From emitted synchrotron radiation we can tell that they contain magnetic fields and cosmic-ray electrons. Since cosmic plasmas must be neutral, there must be also protons or positrons in the jet. Through the jets the synchrotron plasma flows to the lobes: the plasma arriving at the end of the jet is deflected back to form the lobe (a large bubble surrounding the jet). Near the AGN the jets are supersonic (the flow speed is faster than the speed of sound in the jet plasma) and shockwaves form easily, giving rise to small regions with high pressure, which radiate intensely. Further away from the AGN, the weaker jets become subsonic and turbulent. The interaction of

the jet with the ambient can give rise to heating and particle acceleration via shocks, in which thermal and non-thermal radiation is produced.

DRAGNs are characterized by bright hotspots: they are found near the end of each lobe (they are part of the lobes) and they mark the ends of the jets. The "end of the jet" is just the point where the jet collides with the surface of the lobe. If the jet is still supersonic at this point, this collision will take place through a system of strong shockwaves, and the resulting high-pressure region will be seen as the hotspot.

For investigating the spectral index distribution we chose 3C 349 source because it shows dramatic changes of surface brigthness, and also there is a big contrast in the flux at the two ends, as well as flux contrast at two frequencies. Therefore this DRAGN is suitable for physical understanding of the radio source phenomena.

3C 349 source is a Fanaroff-Riley Class II (Fanaroff & Riley 1974) radio galaxy with high luminosity, faint jets but bright hotspots at the ends of the lobes, and it is very powerfull.

2. LEAHY'S ATLAS OF DRAGNs

Leahy's Catalogue of double radio sources can be found at the internet address http://www.jb.man.ac.uk/atlas/. The radio images and other data for the nearest 85 DRAGNs (radio galaxies and related objects), in the so-called "3CRR" sample of Laing, Riley & Longair (1983), are presented.

This atlas, edited by J. P. Leahy, A . H. Bridle, and R. G. Strom, contains all the DRAGNs brighter than a given flux density in a certain region of sky: the brightest DRAGNs in the accessible regions of the northern hemisphere (originally based on the 3CR catalogue - 3^{rd} Cambridge Catalog of Radio Sources). The most common frequencies are near 1.5 GHz, but also there are frequencies ranging from 0.3 to 8.4 GHz.

They have put the Atlas together because modern radio images of the 3C sample were scattered over many papers, making it very difficult to use for systematic analysis. The images in the Atlas have been chosen to given a good overview of the total structure of each DRAGN.

Here we want to stress that this Atlas contains calibrated data, i.e. many programs are used to make final images and data. In the particular case of the 3C 349 source, the methods used are CLEAN and VTESS computational algorithms.

3. DATA AND METHOD

Radio observations that we used in our calculations are obtained by the Very Large Array of the National Radio Astronomy Observatory. At least two frequencies are necessary for determining spectral index, and we use measurements at the two frequencies: at 8414.9 MHz (Hardcastle et al. 1997) and at 1502.4 MHz (Leahy & Perley 1991).

The method of calculation is described in Borka (2007) for Galactic radio loops I-VI, Borka, Milogradov-Turin & Urošević (2008) for Loops V and VI, Borka Jovanović & Urošević (2009) for Monoceros loop, Borka Jovanović & Urošević (2011) for Cygnus and in Borka, Borka Jovanović & Urošević (2011) for HB 21. This method we developed for large radio loops (I-VI), but later on we applied it to angularly large SNRs

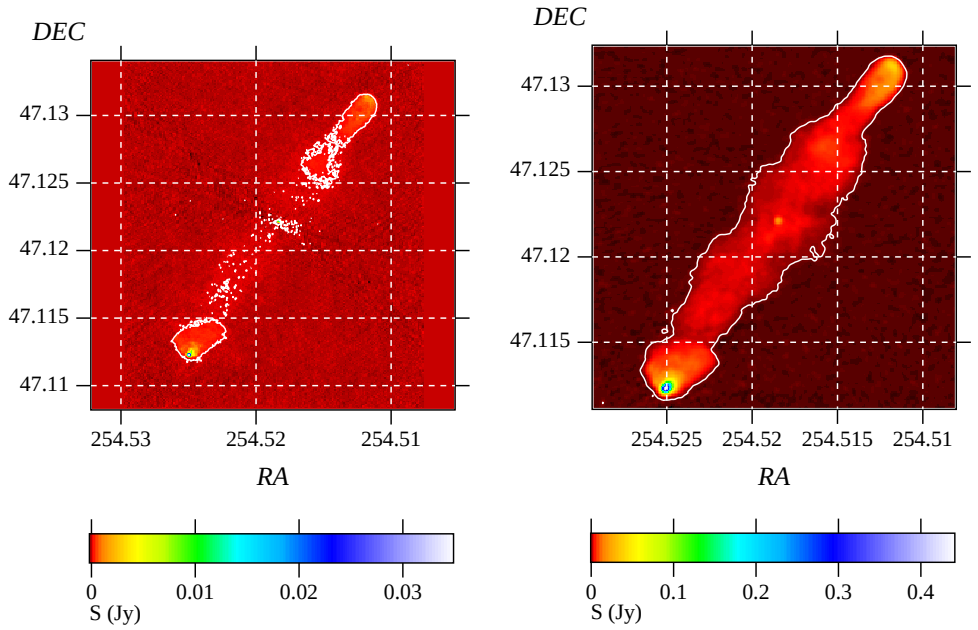

Figure 1: The area of 3C 349 at 8415 MHz (left) and 1502 MHz (right), showing contours of flux density. The contours represent the flux densities $S_{\min} = 9{\times}10^{-5}$ Jy (left) and $S_{\min} = 5{\times}10^{-4}$ Jy (right). The corresponding flux density scales are given (in Jy).

(Monoceros, Cygnus and HB 21) and showed that it is rather efficient in the case of large SNRs. Now we want to extend the same method to extragalactic radio sources.

The dependence between brightness temperature $T_{\mathrm{b},\nu}$, frequency ν and brightness temperature spectral index β is:

$$T_{\mathrm{b},\nu} = K\nu^{-\beta}. \tag{1}$$

As for surface brightness Σ_ν and flux density S_ν it holds $\Sigma_\nu = (2k\nu^2/c^2)T_{\mathrm{b},\nu}$ (where k is the Boltzmann constant and c the speed of light) and $S_\nu = \Sigma_\nu\ \Omega$ (Ω is the solid angle), it is easy to see that the dependence between flux density S_ν, frequency ν and flux density spectral index α would be:

$$S_\nu = K_1\nu^{-\alpha}, \tag{2}$$

where K and K_1 are constants and it holds $\beta = \alpha + 2$. In Leahy's Atlas we deal with flux densities, while in previous cases (Galactic loops) we had brightness temperature data, but because of this linear dependence the same procedure can be used. Extension of this method to much smaller objects is possible because the objects from this atlas are observed with much better resolution. The only difference is that when calculating the flux density, we do not need to consider background radiation as this has already been subtracted. In Fig. 1 it is shown the area of 3C 349, in Equatorial

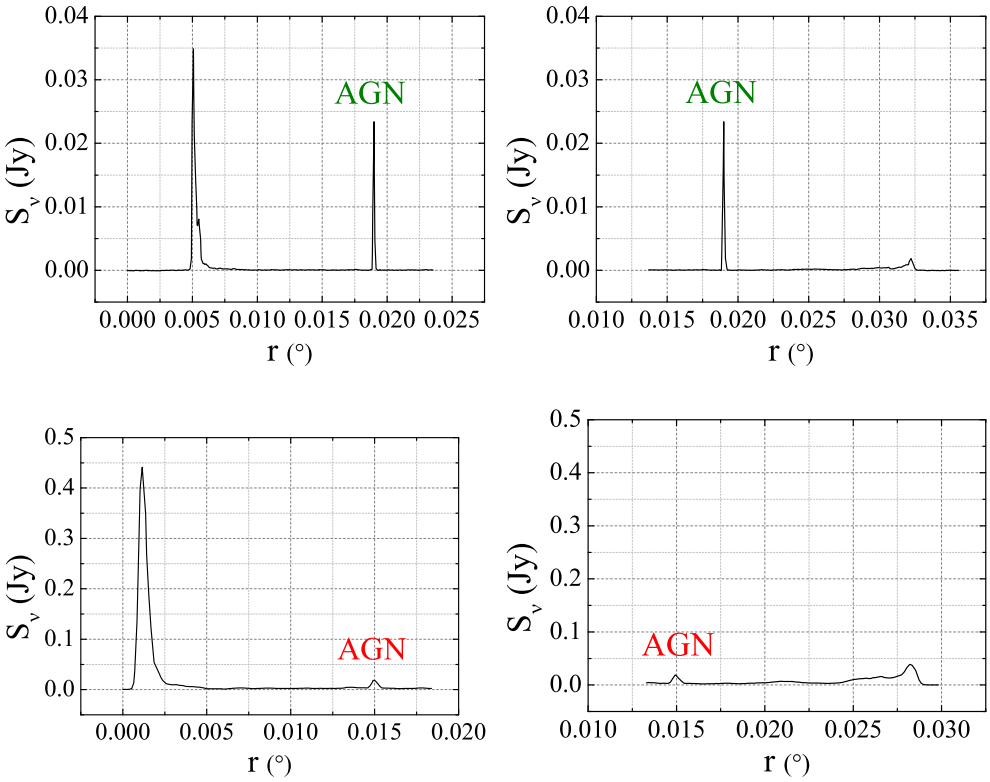

Figure 2: Flux density profiles for 3C 349. Left panel: Southern lobe and AGN. Right panel: Northern lobe and AGN. Top panel is for 8415 MHz, and the bottom panel is for 1502 MHz. In all figures, r (°) would be axis between AGN and the center of the given lobe.

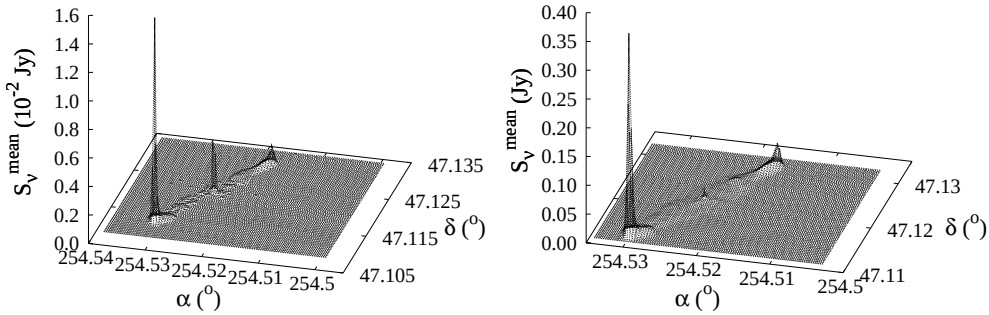

Figure 3: Mean flux histogram for 3C 349 at 8415 MHz (left) and 1502 MHz (right).

coordinates, with contour for minimal flux density $S_{\min}$, which is the border between source and the background. The minimal flux densities are: 9×10^{-5} Jy at 8415 MHz and 5×10^{-4} at 1502 MHz. We presented flux density profiles in Fig. 2, from where

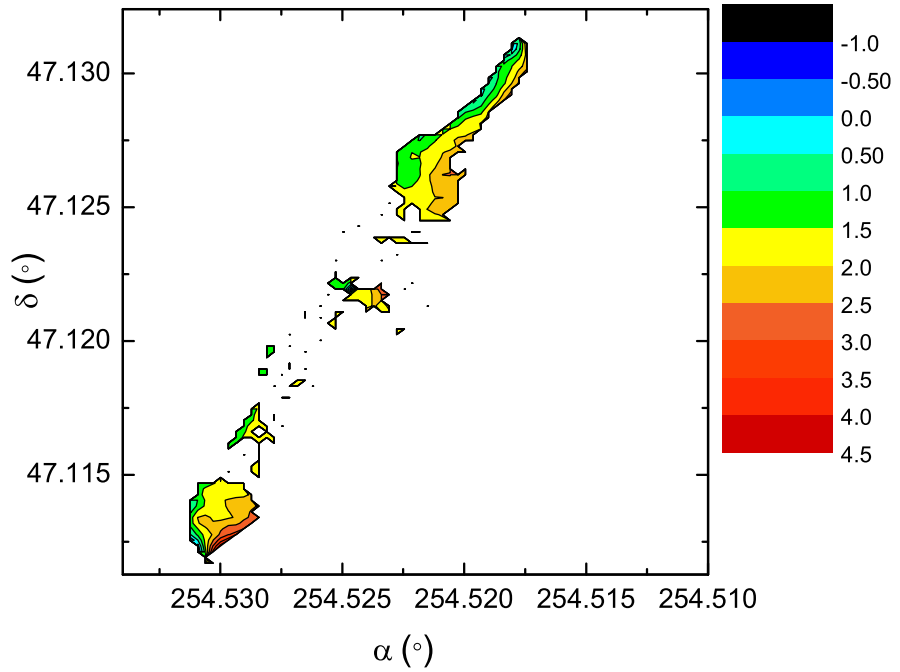

Figure 4: Distribution of radio spectral index for 3C 349 between 8415 and 1502 MHz.

the flux densities of the components (Northern lobe, AGN and Southern lobe) can be read. Our calculated values agree well with those given by Jenkins, Pooley and Riley (1977) at 5 GHz (part of the Table 1 in page 93, column 10), but we think that our method is more precise. The values of flux densities for the northern hotspot, AGN and southern hotspot are the following: (a) 0.001846, 0.0234 and 0.03487 Jy at 8415 MHz; (b) 0.03892, 0.01854 and 0.44109 Jy at 1502 MHz (respectively). For our analysis of flux density, we used the experimental data: for 8415 MHz frequency we sampled values in 11 337 points, and for 1502 MHz frequency in 12 560 points.

If we present spectrum using Eq. (2), then from:

$$\log S_\nu = \log K_1 - \alpha \log \nu \tag{3}$$

we can find radio spectral index as negative value of coefficient of the line. We used the spectral index to study the radiation mechanisms of radio sources.

4. RESULTS AND CONCLUSIONS

For extragalactic radio source 3C349 we calculated flux densities over its area. The area of this radio source was divided into more bins and we calculated mean fluxes for every bin. Using bins with the same coordinates at two frequencies, from spectrum (flux density as a function of frequency) we obtained spectral indices α. Like shown in Eq. (3), the spectral index is calculated as negative value of the line's coefficient. So we used spectral index to study the radiation mechanism of radio sources. The mean flux histograms at 8415 and 1502 MHz are shown in Fig. 3. From Figs. 2 and

3 we can also read the flux densities of the both radio lobes and AGN (which is in the center). For the 8415 MHz frequency, the southern lobe has greater flux density than the AGN but for the northern lobe it is opposite. At 1502 MHz, it is noticeable that the southern lobe has greater flux density than the AGN, while the northern lobe also has greater flux density than the AGN but this difference is less.

Distribution of radio spectral indices is a useful tool for studying the nature of radio emission of extended extragalactic radio sources. Radio spectral index for 3C 349 and radiation characteristics can be seen from Fig. 4. The spectral indices of the following points: in the center (AGN), one point in one lobe (just where the hotspot is) and one point in another lobe (also hotspot) denote thermal radiation. Except this, over the area of the observed source, indices are all greater than 0.1, which denotes non-thermal radiation. Beside conclusion about nature of radiation, from Fig. 4 it can be seen what the α distribution is like. It is noticeable that along the jet the spectral indices are similar.

From our calculations it can be noticed that our method developed for Galactic radio loops, could be applicable to the extragalactic radio sources, too. By use of that method we calculated spectral index distribution of 3C 349 between 1502.4 and 8414.9 MHz. Obtained spectral index variation for this source shows that: (1) non-thermal (synchrotron) radiation dominates over the whole source except its core (active nucleus) and hot spots in the radio lobes, (2) thermal radiation is responsible for high brightness of the hot spots in the both lobes of the 3C 349 source.

Acknowledgments

This research is part of the project 176003 "Gravitation and the large scale structure of the Universe" supported by the Ministry of Education and Science of the Republic of Serbia.

References

Borka, V.: 2007, *Mon. Not. R. Astron. Soc.*, **376**, 634.
Borka, V., Milogradov-Turin, J., Urošević, D.: 2008, *Astron. Nachr.*, **329**, 397.
Borka Jovanović, V., Urošević, D.: 2009, *Astron. Nachr.*, **330**, 741.
Borka Jovanović, V., Urošević, D.: 2011, *Rev. Mex. AA*, **47**, 159.
Borka, D., Borka Jovanović, V., Urošević, D.: 2012, *Rev. Mex. AA*, **48**, 53.
Fanaroff, B. L., Riley, J. M.: 1974, *Mon. Not. R. Astron. Soc.*, **167**, 31P.
Hardcastle, M. J., Alexander, P., Pooley, G. G., Riley, J. M.: 1997, *Mon. Not. R. Astron. Soc.*, **288**, 859.
Jenkins, C. J., Pooley, G. G., Riley, J. M.: 1977 *Mem. R. Astron. Soc.*, **84**, 61.
Laing, R. A., Riley, J. M., Longair, M. S.: 1983, *Mon. Not. R. Astron. Soc.*, **204**, 151.
Leahy, J. P., Perley, R. A.: 1991, *Astron. J.*, **102**, 537.
Leahy, R. A.: 1993, *Lecture Notes in Physics*, **421**, 1.